



# A global analysis of agricultural productivity and water resource consumption changes over cropland expansion regions

Zhengjia Liu<sup>a,b,\*</sup>, Yansui Liu<sup>a,b</sup>, Jieyong Wang<sup>a,b,\*</sup>

<sup>a</sup> Key Laboratory of Regional Sustainable Development Modeling, Institute of Geographic Sciences and Natural Resources Research, Chinese Academy of Sciences, Beijing 100101, China

<sup>b</sup> College of Resources and Environment, University of Chinese Academy of Sciences, Beijing 100049, China

## ARTICLE INFO

### Keywords:

Global cropland expansion  
Agricultural productivity  
Water resource consumption  
Land use change  
Spatial analyses

## ABSTRACT

Cropland expansion often occurs on grasslands and partial forests. However, there is little quantified understanding of how cropland expansion affected the agricultural productivity and water resource consumption globally. In this study, we used spatially explicit satellite-based data, including land use maps, net primary productivity and evapotranspiration from 2001 to 2018, and the space-for-time substitution technique to investigate the relationships between cropland expansion and agricultural productivity and water resource consumption. Results showed that global cropland area presented a significant net increasing trend with  $1.9 \times 10^4 \text{ km}^2/\text{a}$  ( $p < 0.01$ ) since 2000. Net increased cropland area over the Northern Hemisphere and the Southern Hemisphere occupied 27.1% and 72.9% of global total net increase, respectively. Large-area cropland expansion mainly focused on Eastern Asia, Southern Asia, Eastern Europe, Southern America, and Northern America. Particularly, cropland expansion in the Southern America deserved the greatest attention. At the global scale, new expanded croplands caused average NPP decrease and average ET decrease compared to original ecosystems, but performances were evident differences in subregions. Cropland expansion in the Southern America evidently decreased NPP and ET compared to other places. In contrast, new expanded croplands in most subregions of Asia and Northern America performed higher the agriculture productivity, while the increases were done at the expense of more water resource consumption. Although cropland expansion only slightly decreased NPP compared to original ecosystems globally, new expanded croplands often occurred in water-limited or temperature-limited areas according to precipitation and temperature gradations. This study suggests that cropland expansion should more consider sustainable land use and development, and reduce the risks of cropland expansion on natural ecosystems as much as possible.

## 1. Introduction

Croplands are expanded to compensate for the food-energy-fiber requirements of increasing population and to offset the cropland decrease due to urban expansion accounting for peri-urban croplands (d'Amour et al., 2017; Foley et al., 2011). Globally, cropland expansion has led to the transformation of many landscapes from natural ecosystems to agricultural ecosystems, and further modified habitat, land cover and carbon-water-energy balance (Ewers et al., 2009; Folberth et al., 2020; Foley et al., 2005; Li et al., 2020a). Previous studies documented that land reclamation largely occurred on grasslands and partial forests, e.g., Amazon Forest region, Eurasian grassland region

and sub-Sahara Africa (Tan and Li, 2019; Zaveri et al., 2020). While cropland expansion status and its driving factors have been widely studied, there is little quantified understanding of how global cropland expansion affected the agricultural productivity and water resource consumption.

Net primary productivity (NPP) and evapotranspiration (ET) are two important indicators for representing vegetation productivity and water resource consumption. Process-based ecosystem/land-surface models and in-situ measurement experiments, providing estimated NPP and ET fluxes, are often employed to forecast the impacts of land use changes on vegetation productivity and water resource consumption (Tao et al., 2003; Yan et al., 2009). However, there are two respective limitations

\* Corresponding authors at: Key Laboratory of Regional Sustainable Development Modeling, Institute of Geographic Sciences and Natural Resources Research, Chinese Academy of Sciences, Beijing 100101, China.

E-mail addresses: [liuzj@igsnr.ac.cn](mailto:liuzj@igsnr.ac.cn) (Z. Liu), [liuys@igsnr.ac.cn](mailto:liuys@igsnr.ac.cn) (Y. Liu), [wjy@igsnr.ac.cn](mailto:wjy@igsnr.ac.cn) (J. Wang).

<https://doi.org/10.1016/j.agee.2021.107630>

Received 30 June 2021; Received in revised form 4 August 2021; Accepted 16 August 2021

Available online 26 August 2021

0167-8809/© 2021 Elsevier B.V. All rights reserved.

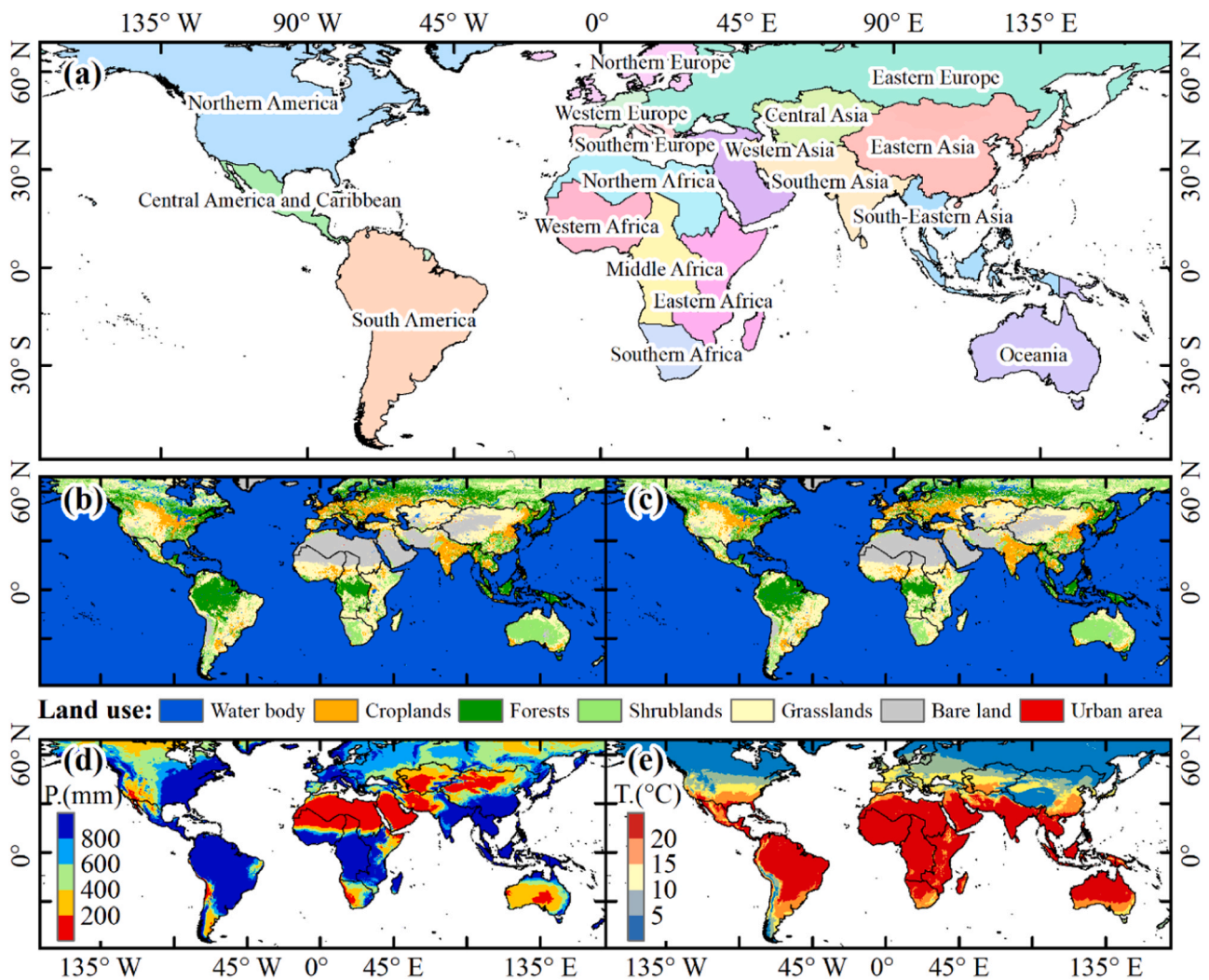


**Fig. 1.** Global 18 subregions (a), land use/cover data and climate data used in this study. Sub-figures (b) and (c) denote land use patterns based on five-year majority cell grid statistics in 2001–2005 and in 2014–2018; sub-figures (d) and (e) denote multi-year average patterns of total precipitation (P.) and air temperature (T.) from 2001 to 2018.

for above approaches. First, cropland expansion often occurs on small patches and could take a long time to reach a relatively large area. Coarse-resolution climate data-based models are, thus, often difficult to capture the effects of cropland expansion in view of uncertainty impacts of the input data on estimated NPP and ET fluxes (Gu et al., 2017; Mo et al., 2009). By contrast, in-situ measurement experiments can capture the refined variations of carbon and water fluxes induced by land reclamation, but sparse spatial samplings make its ability poor at a large-area scale (Niu et al., 2021).

Some spatially explicit global NPP and ET products have been derived (Gu et al., 2017; Jiang and Ryu, 2016; Matsushita et al., 2004; Running et al., 2004). Compared to coarse resolution products derived from process-based models and in-situ measurement experiments, remote sensing products can provide relatively finer spatial NPP and ET information. In remote sensing products, MODIS NPP and ET products were widely used owing to features with good spatial resolution, open access and good timeliness (Mu et al., 2012; Running et al., 2004; Zhao et al., 2005). However, note that remote sensing products gave expression to the actual NPP and ET, that is, not only reflecting the impacts of the human activities, but also including the effects of climatic factors and CO<sub>2</sub> fertilization (Liu et al., 2020). Therefore, how to separate the impacts of cropland expansion on agricultural productivity and water resource consumption is challenging. To answer this question, we first

need to find where are potential cropland expansion located? Some previous studies investigated global cropland change and its causes (Tan and Li, 2019; Zaveri et al., 2020). For example, a recent study from Tan and Li (2019) used European Space Agency (ESA) Climate Change Initiative (CCI) land cover products with United Nations (UN) classification to analyze annual trends and spatiotemporal variations in cropland area globally during 1992–2015. Based on ESA CCI land cover products as well as MODIS land cover products (MCD12Q1), Zaveri et al. (2020) indicated that rainfall anomalies were a significant driver of cropland expansion. Still, cropland expansion patterns are less well understood, and are yet to be quantified at the global and continental scales. Second, when we quantify the contributions of cropland expansion on agricultural productivity and water resource consumption, simulation based on process-based model with scenario experiments could be the usual approach. Yet this approach could suffer from a big challenge due to its coarse spatial resolution as the above mentioned. Fortunately, the space-for-time substitution technique could be the alternative approach. The space-for-time substitution technique assumes that spatial and temporal variations are equivalent (Pickett, 1989). Specifically, assuming two spatial adjacent regions A and B with similar water-soil-temperature environments have the same land use type, i.e., grasslands, ten years ago. The land use type in region A was converted into croplands before five years. At present, by comparing the

certain indicator changes of regions A and B, we can easily measure the environmental effects of conversion from grasslands to croplands. Besides, after we understand the contributions of cropland expansion on agricultural productivity and water resource consumption, what are the significances of these findings in different geospatial regions or continents that are urgently clarified. These questions play very crucial roles in regional agriculture-water management and sustainable human-land-environment development.

Therefore, the study tries to fill the above-mentioned knowledge gaps by addressing the following questions: (1) Where are the most rapid cropland expansion areas at the past two decades? (2) What are the responses of agricultural productivity and water resource consumption to cropland expansion? and (3) discuss the significances of these findings for sustainable land use and regional agriculture development?

## 2. Data and methods

### 2.1. Data collections

Annual satellite-based MODIS NPP, ET and land cover data with spatial resolution of 500-m were used in this study. We collected these data from the website of Application for Extracting and Exploring Analysis Ready Samples (AppEARS, [https://lpdaacsvc.cr.usgs.gov/app\\_eears/](https://lpdaacsvc.cr.usgs.gov/app_eears/)). This study acquired the data in the geographic coordinate projection system (WGS-84). The ERA5 precipitation and temperature data were collected from European Centre for Medium-range Weather Forecasts (ECMWF, <https://www.ecmwf.int/en/forecasts/datasets/reanalysis-datasets/era5>). The boundaries of global and 18 subregions were collected from natural Earth vectors datasets of ENVI software (Fig. 1).

Yearly global land cover types in 2001–2018 were acquired from MCD12Q1 version 6 data product. It was derived from six different classification schemes, covering International Geosphere-Biosphere Programme (IGBP) classification, University of Maryland (UMD) classification, Leaf Area Index (LAI) classification, BIOME-Biogeochemical Cycles (BGC) classification, Plant Functional Types classification, and FAO-Land Cover Classification System 1 land cover layer. The classification products are derived by using supervised classification approach as well as MODIS Terra and Aqua reflectance information (Friedl et al., 2002). Besides, additional post-processing, including prior knowledge and ancillary information, was used to further refine specific classes. We extracted the cropland distribution data from IGBP layer of the MCD12Q1 version 6 product in view of wide use of the IGBP classification system. The original IGBP layer includes 17 land cover classes. To make it easier to graphics display, The IGBP land cover classes were generalized by aggregating the 17 classes into 7 major land cover types, i.e., forests, shrublands, grasslands, croplands, urban area, bare land, and water body.

Yearly NPP data in 2001–2018 were acquired from the MOD17-A3HGF Version 6.1 product. Annual NPP is derived from the sum of all 8-day net photosynthesis products (MOD17A2H) from the given year. The net photosynthesis value is the difference of the gross primary productivity and the maintenance respiration (Running et al., 2004; Zhao et al., 2005). The gap-filled MOD17A3HGF is an improved MOD17 product compared to those of previous versions, because it has cleaned the poor-quality inputs, e.g., good-quality leaf area index and fraction of photosynthetically active radiation (Liu et al., 2015).

Yearly ET data in 2001–2018 were acquired from MOD16A2GF Version 6.1 Evapotranspiration/Latent Heat Flux (ET/LE) product. This product is the sum of all gap-filled 8-day dataset within the composite period. Each 8-day data is derived from the logic of the Penman-Monteith equation (Mu et al., 2011). Input data of the algorithm include daily meteorological reanalysis data, MODIS remotely sensed vegetation property dynamics, albedo, and land cover. Like MOD17-A3HGF, the gap-filled MOD16A2GF is the improved MOD16 product.

The ERA5 precipitation and air temperature data are spatial

resolution of 0.1°. In order to investigate the impacts of cropland expansion on agricultural productivity and water source consumption in different precipitation and temperature gradients, this study computed the multi-year averages of annual total precipitation and annual mean air temperature in 2001–2018.

### 2.2. Processing and statistical analyses

To reduce the uncertainties of cropland distribution data, this study derived two new composite cropland data based on MODIS IGBP cropland datasets. Namely, we used the two five-year land cover data (i.e., 2001–2005 and 2014–2018) to derive cropland data in the two periods (Y2001–2005 and Y2014–2018), respectively. Specifically, for each pixel, if its land cover types in five years are all croplands, the corresponding pixel of the new composite dataset is assigned croplands, otherwise non-croplands. Like cropland composite, this study also derived other six land cover map in the Y2014–2018 period. This assumption thus ignored short-term land use changes. The aim of this study is to monitor the impacts of cropland expansion on agricultural productivity and water source consumption, which is, after all, a relatively long-run effect. Subsequently, we aggregated the two ~500-m cropland maps into percent cropland maps with spatial resolution of 0.1 latitude and longitude cell grid. We obtained the changes of Y2001–2005 croplands and Y2014–2018 croplands.

Cropland expansion areas in this study were defined as regions with cropland increased area being greater than 10% for each 0.1 latitude and longitude cell grid. We expected that the given 0.1 cell grid had more 500-m cropland expansion pixels in order to reduce the uncertainty of data statistics. The net cropland increase denotes the residue than cropland gain (or expansion) minus cropland loss in the given region. To investigate the impacts of cropland expansion on agricultural productivity and water resource consumption and to reduce the impacts from other factors (e.g., climate change), the following steps were done.

Step1: This study calculated the averaged values of each pixel in 2014–2018 for ~500-m NPP and ET data. The aim is to obtain the normal NPP and ET status of vegetation and to reduce the impacts of extreme events as much as possible.

Step2: Based on locations of cropland increased area being greater than 10% for each 0.1 latitude and longitude cell grid (regarded as cropland expansion areas in this study), we counted changes, numbers, and values on ~500-m land use type, NPP and ET in each 0.1-degree cell grid. In this step, some changed information were collected for each 0.1-degree cell grid, including what being the original land use type before conversion into croplands, which land use type being the best major conversion into croplands, and related information. Take the major land use type being grasslands in the given 0.1-degree cell grid as an example. Collected information covered the numbers and locations of the inflexible grasslands in the ~500-m Y2014–2018 map, corresponding averaged grassland NPP and ET values ( $NPP_{\text{grasslands, Y2014-2018}}$  and  $ET_{\text{grasslands, Y2014-2018}}$ ), the numbers and locations of new croplands in the ~500-m Y2014–2018 map but being grasslands in the ~500-m Y2001–2005 map, corresponding averaged new cropland NPP and ET values ( $NPP_{\text{new-croplands, Y2014-2018}}$  and  $ET_{\text{new-croplands, Y2014-2018}}$ ).

Step3: We computed the difference of  $NPP_{\text{new-croplands, Y2014-2018}}$  and  $NPP_{\text{grasslands, Y2014-2018}}$  (taking grasslands as an example again), and the difference of  $ET_{\text{new-croplands, Y2014-2018}}$  and  $ET_{\text{grasslands, Y2014-2018}}$ , respectively.

$$\Delta NPP = NPP_{\text{new-cropland, Y2014-2018}} - NPP_{i, Y2014-2018} \quad (1)$$

$$\Delta ET = ET_{\text{new-cropland, Y2014-2018}} - ET_{i, Y2014-2018} \quad (2)$$

where,  $NPP_{\text{new-croplands, Y2014-2018}}$  and  $ET_{\text{new-croplands, Y2014-2018}}$  are averaged new cropland NPP and ET values in the Y2014–2018 map for the given 0.1-degree cell grid.; the subscript  $i$  represents the given original land use type, e.g., grasslands in the above-mentioned example;  $NPP_{i, Y2014-2018}$  and  $ET_{i, Y2014-2018}$  are averaged NPP and ET values of



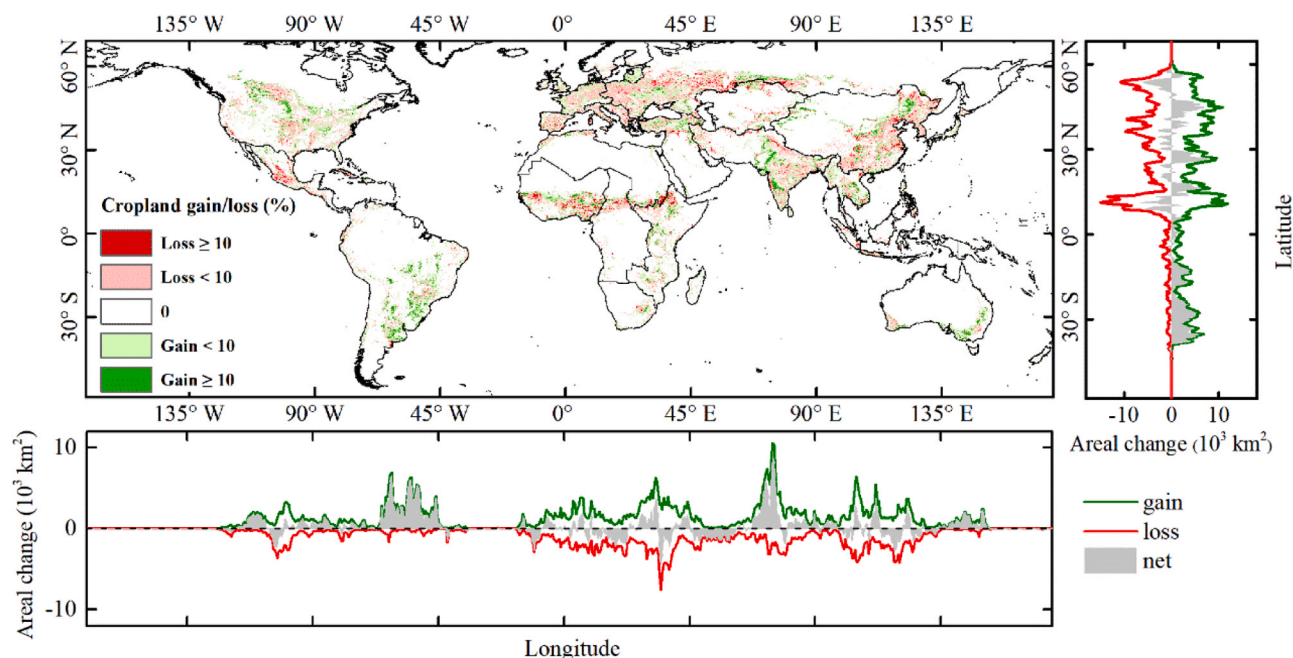


Fig. 2. Distributions of cropland gain and loss based on five-year majority land use type maps from 2001 to 2005 and 2014–2018.

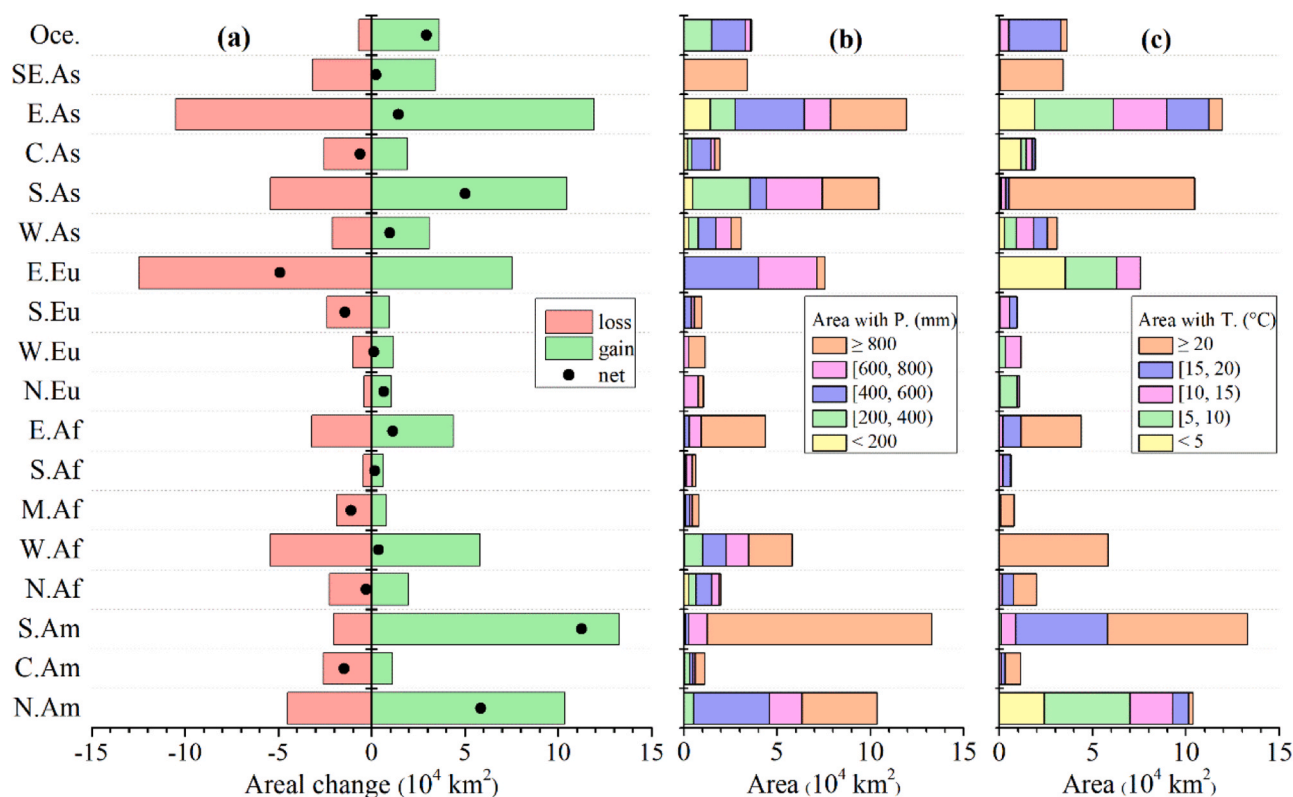
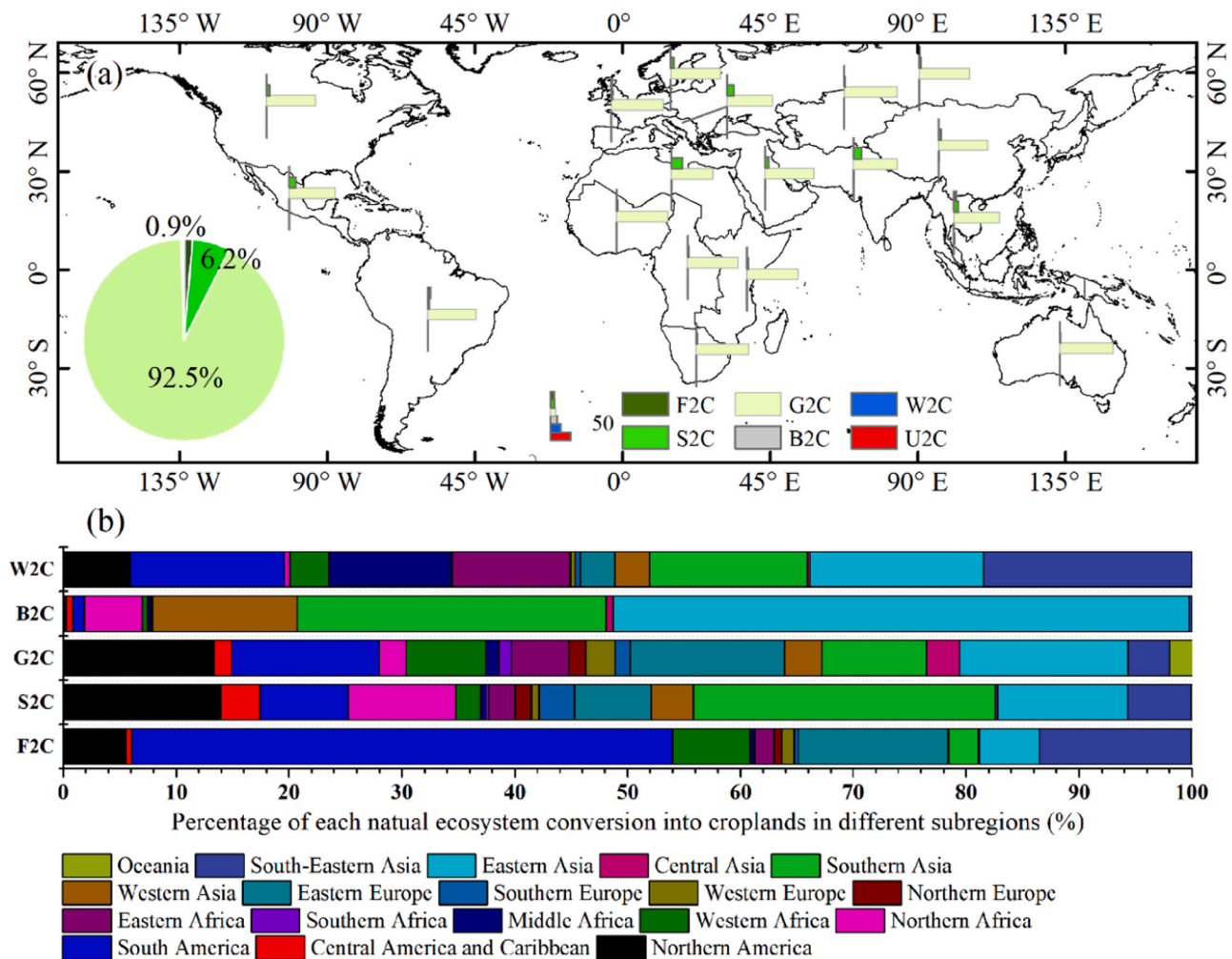


Fig. 3. Cropland gain, loss and net areal change in different subregions (a), and cropland expansion area along with (b) total precipitation gradients (mm) and (c) mean air temperature gradients ( $^{\circ}\text{C}$ ).

the inflexible land use type  $i$  in the Y2014–2018 map for the given 0.1-degree cell grid. Note that  $\Delta\text{NPP}$  and  $\Delta\text{ET}$  were regarded as the impact of cropland expansion on agricultural productivity and water source consumption in the given 0.1-degree cell grid within the conceptual framework of the space-for-time substitution technique (Pickett, 1989). By using the approach, this study computed  $\Delta\text{NPP}$  and  $\Delta\text{ET}$  of all

0.1-degree cell grids with cropland increased area being greater than 10%. In particular, the space-for-time substitution technique largely reduced the time effects of climate change and atmospheric  $\text{CO}_2$  fertilization on NPP and ET as the Introduction section explored. Besides, patterns of cropland expansion,  $\Delta\text{NPP}$  and  $\Delta\text{ET}$  along with precipitation and temperature were also investigated. Multi-year mean precipitation



**Fig. 4.** Percentage of natural ecosystems conversion into croplands in the globe and each subregion (a), and percentage of each natural ecosystem conversion into croplands in subregions (b). F2C, S2C, G2C, B2C and W2C note forests (F), shrubland (S), grasslands (G), bare land (B) and water body (W) conversion into croplands, respectively.

was classified five gradients, i.e., P1: < 200 mm, P2: 200–400 mm, P3: 400–600 mm, P4: 600–800 mm and P5:  $\geq 800$  mm. Also, multi-year mean air temperature was classified five gradients, i.e., T1: < 5 °C, T2: 5–10 °C, T3: 10–15 °C, T4: 15–20 °C and T5:  $\geq 20$  °C.

### 3. Results

#### 3.1. Characteristics of global cropland expansion

Global cropland area presented a significant net increasing trend with  $1.9 \times 10^4$  km<sup>2</sup>/a ( $p < 0.01$ ) over the past two decades, increasing from  $12.8 \times 10^6$  of average in 2001–2005– $13.1 \times 10^6$  km<sup>2</sup> of average in 2014–2018 according to statistics of the MODIS IGBP land use and land cover maps (Fig. 2). Net increased cropland area over the Northern Hemisphere and the Southern Hemisphere accounted for 27.1% and 72.9% of global total net increase, respectively. At the continental and corresponding subregion scale, South America ( $11.2 \times 10^4$  km<sup>2</sup>), Northern America ( $5.8 \times 10^4$  km<sup>2</sup>), Southern Asia ( $5.0 \times 10^4$  km<sup>2</sup>) and Oceania ( $2.9 \times 10^4$  km<sup>2</sup>) had the largest net cropland increase (Fig. 3a). Brazil, India, United States of America, Argentina, Australia, Canada, China, Pakistan, Turkey and Ukraine were the top ten net increased countries, and their net cropland increased area all overpassed  $7 \times 10^3$  km<sup>2</sup>.

Different from a single mode of cropland expansion in the Southern Hemisphere, modes of cropland change over the Northern Hemisphere

were more complex. Cropland area in some regions showed net decrease due to much cropland loss, especially in 7–13°N and 50–55°N. By contrast, cropland area in some regions (e.g., 55–57°N, 37–50°N, 35–30°N, 13–18°N, and 0–7°N) also presented evidently net increase because of much greater cropland expansion. Although the Northern Hemisphere only had relatively low net cropland increase amount, its cropland expansion accounted for 74.3% of total cropland expansion. At the continental and corresponding subregion scale, South America ( $13.7 \times 10^4$  km<sup>2</sup>), Eastern Asia ( $11.9 \times 10^4$  km<sup>2</sup>), Northern America ( $10.4 \times 10^4$  km<sup>2</sup>), Southern Asia ( $10.5 \times 10^4$  km<sup>2</sup>), Eastern Europe ( $7.6 \times 10^4$  km<sup>2</sup>) and Western Africa ( $5.8 \times 10^4$  km<sup>2</sup>) performed evident cropland expansion phenomenon. China, India, United States of America, Brazil, Russia, Argentina, Australia, Canada, Nigeria and Turkey were the top ten cropland expansion countries, and their expansion area all overpassed  $1.5 \times 10^4$  km<sup>2</sup>.

Meanwhile, this study observed that 85.9% of global cropland expansion were largely located in regions with annual total precipitation being greater than 400 mm (i.e., semi-humid and humid regions). Particularly, for subregions with evidently cropland expansion, Southern America, Eastern Asia, Southern Asia, Northern America, Eastern Europe, Western Africa and Eastern Africa separately had 99.3% ( $13.3 \times 10^4$  km<sup>2</sup>), 76.8% ( $11.9 \times 10^4$  km<sup>2</sup>), 66.1% ( $10.5 \times 10^4$  km<sup>2</sup>), 95.0% ( $10.4 \times 10^4$  km<sup>2</sup>), 99.4% ( $7.6 \times 10^4$  km<sup>2</sup>), 82.8% ( $5.8 \times 10^4$  km<sup>2</sup>) and 99.0% ( $4.4 \times 10^4$  km<sup>2</sup>) areas locating in the semi-humid and humid regions (Fig. 3b). Of course, this study also found that there were

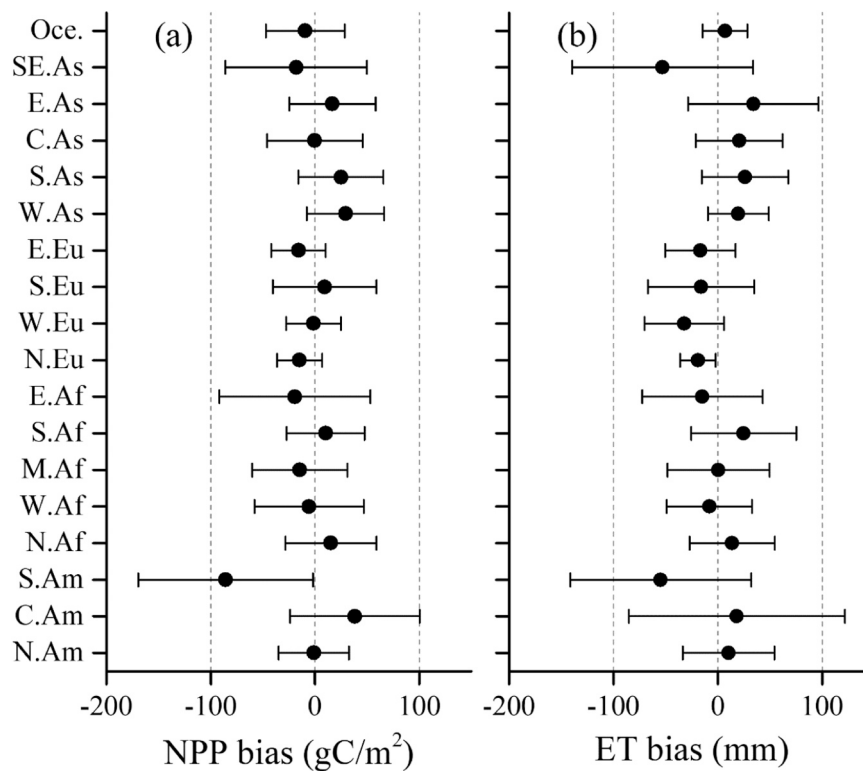


Fig. 5. Changes of net primary productivity (NPP, a) and water resource consumption (ET, b) responses to cropland expansion in different subregions.

the water-limited areas having abundant cropland expansion in some subregions. For example, Eastern Asia, Southern Asia and Western Africa separately had 23.2% ( $2.8 \times 10^4 \text{ km}^2$ ), 33.9% ( $3.5 \times 10^4 \text{ km}^2$ ) and 17.2% ( $1.0 \times 10^4 \text{ km}^2$ ) areas locating in the semi-arid and arid regions. Cropland expansion regions with annual mean temperature being lower than  $10^\circ\text{C}$  covered 51% ( $6.1 \times 10^4 \text{ km}^2$ ), 67.6% ( $7.0 \times 10^4 \text{ km}^2$ ) and 83% ( $6.3 \times 10^4 \text{ km}^2$ ) of total cropland expansion in Eastern Asia, Northern America and Eastern Europe (Fig. 3c), respectively.

Global cropland expansion mainly occupied grasslands ( $\sim 92.5\%$  of newly croplands), followed by shrublands (6.19%), forests (0.91%), bare land (0.29%) and water body (0.13%). Regions with shrublands being converted into croplands mainly concentrated into Southern Asia, especially in northwestern India. Regions with forests being converted into croplands mainly concentrated Southern America, especially in Argentina, Bolivia and Brazil. Regions with bare land being converted into croplands mainly focused upon Eastern Asia and Southern Asia, especially in northwestern China (Fig. 4).

### 3.2. Responses of agricultural productivity and water resource consumption to cropland expansion at global and regional scales

Cropland expansion slightly caused global average NPP decrease ( $-12.8 \text{ gC/m}^2$ ) and average ET decrease ( $-4.0 \text{ mm}$ ) of new cultivated land pixels, but difference performances were evidently observed in subregions (Fig. 5). Cropland expansion tended to increase regional average NPP and ET in Central America and Caribbean, Northern Africa, Southern Africa, Western Asia, Southern Asia and Eastern Asia. Particularly, Central America and Caribbean performed the strongest NPP increase with  $38.2 \pm 62.0 \text{ gC/m}^2$ , and Eastern Asia performed the strongest ET increase with  $34.0 \pm 62.5 \text{ mm}$ . In contrast, cropland expansion was inclined to decrease regional average NPP and ET in Southern America, Western Africa, Eastern Africa, Northern Europe, Western Europe, Eastern Europe and Southeastern Asia. Note that Southern America showed the strongest NPP decrease with  $-85.9 \pm 83.7 \text{ gC/m}^2$ , and Southern America and Southeastern Asia both

gave the strongest ET decreases with  $-54.9 \pm 86.6 \text{ mm}$  and  $-53.0 \pm 86.7 \text{ mm}$ , respectively. Besides, there were some subregions displaying diverse signals in average NPP and ET. Cropland expansion in Southern Europe increased NPP but decreased ET. However, cropland expansion in Northern America, Middle Africa, Southern Europe, Central Asia and Oceania slightly decreased NPP but increased ET.

Cropland expansion usually decreased NPP and ET in most areas with high annual total precipitation and high annual mean temperature in Southern America (Fig. 6). Visibly decreased ET phenomenon in areas with high annual total precipitation and high annual mean temperature were also found in Southeastern Asia. In Eastern Asia, water-limited and temperature-limited cropland expansion areas with annual total precipitation being lower than  $600 \text{ mm}$  and annual mean temperature being lower than  $15^\circ\text{C}$  presented observably increased ET (Figs. S1h and S2h), although only slightly increased NPP compared to original land use types (Figs. S3h and S4h). By contrast, NPP and ET change induced by cropland expansion in the rest of subregions were not evident, that is, cropland expansion did not observably alter carbon storage and water consumption amounts at any precipitation and temperature gradients compared to original land use types.

## 4. Discussion

Most expanded croplands largely occurred on marginal land at the global and regional scales, and they very likely suffered from potential risks from climate changes and land degradation. Because most expanded croplands faced limited natural or managerial conditions, such as poor soil fertility, low agriculture management, and limitations from temperature, water source supply or transportation (Kuang et al., 2021; Lesk et al., 2016; Lobell et al., 2008; Schmidhuber and Tubiello, 2007). For example, most expanded croplands were restricted by water resource in Eastern Asia, Northern Asia, Eastern Europe, Western Africa, and Northern America. Some expanded croplands were restrained by relatively low temperature in Eastern Asia, Eastern Europe, and Northern America, due to locating in relatively high latitude. Meanwhile, in



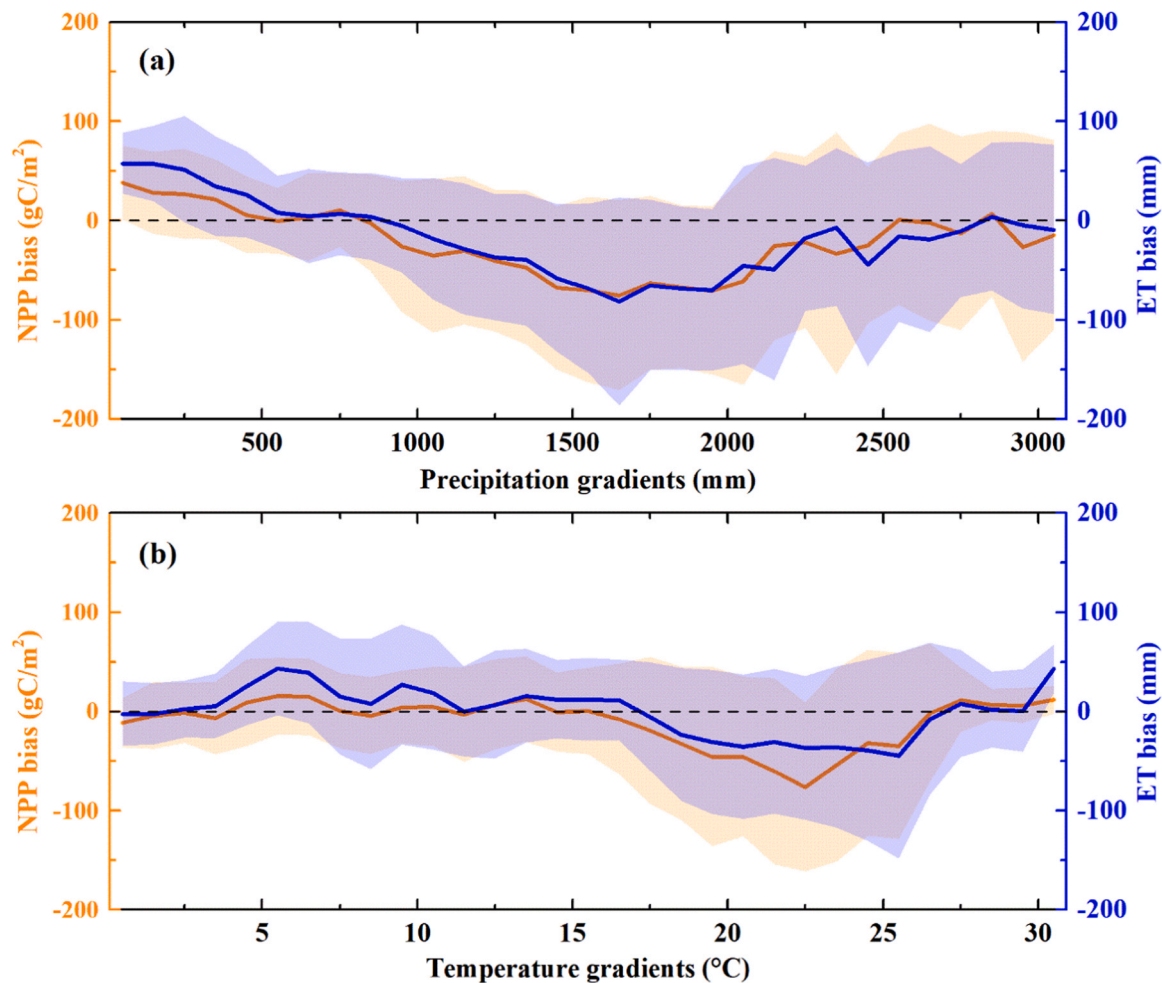


**Fig. 6.** Changes of net primary productivity (NPP) and evapotranspiration (ET) induced by cropland expansion along with precipitation gradients (a) and temperature gradients (b), respectively.

most of these regions, slightly lower temperature could be greatly responsible for regional agriculture development compared to water resources. Therefore, climatic settings and changes are mostly regarded as one of the most important factors for cropland expansion (Zaveri et al., 2020). On the one hand, current warming climate and increased precipitation frequency could be benefit for potentially improving the agricultural productivity and agricultural development potentials in some water resource or temperature limited regions to some extent, and thus largely improve the possibility of cropland expansion in those regions (Dong et al., 2016; Liu et al., 2021, 2019; Liu and Liu, 2018). Dong et al. (2016) reported that paddy rice centroid northward expanded nearly 310 km in Northeastern Asia during the year of 2000–2014. On the other hand, extreme weather events, i.e., droughts, floods, and extreme temperature, could also lead to an increase in cropland expansion (Iizumi and Ramankutty, 2015; Ortiz-Bobea et al., 2021; Zaveri et al., 2020). The earlier hypotheses implied that climate change contributed more to cropping area expansion in higher latitudes and altitudes, but the quantified impacts of extreme weather events on cropland expansion were less studied (Iizumi and Ramankutty, 2015). A recent study found that repeated dry anomalies lead to cropland expansion increase, especially in developing countries, because small-holder farmers could be in response to reduced yields (Zaveri et al., 2020). Their estimates reported that dry anomalies occupied nearly 9% of the rate of cropland expansion at the past two decades. Climate change is, thus, both a challenge and an opportunity for cropland expansion.

The new expanded croplands account for large-area natural

ecosystems, especially in grasslands, shrublands/savanna, and forests. Cropland expansion into fragile ecosystems has exerted even negative effects on carbon sequestration, biodiversity, animal habitat, and ecosystem services in most regions globally (Ewers et al., 2009; Li et al., 2020b; West et al., 2010). In this study, we found that Southern America had the largest-area cropland expansion and the cropland expansion evidently reduced the NPP. Cropland expansion also decreased original ecosystem NPP in Western Africa, Middle Africa, Eastern Africa, and Southeastern Asia where belongs to the tropics. These findings are consistent with the most previous studies (Foley et al., 2011; West et al., 2010). For example, a study from West et al. (2010) investigated the balance between carbon stocks and crop yield on agricultural land, and reported that cropland expansion in tropical landscapes often got relatively poor benefit compared to the cost of carbon stocks. Foley et al. (2011) also indicated that regions of tropical agriculture had a relatively high yield, particularly in regions with sugarcane, oil palm and soybeans, but less contributed to global total calorie and protein supplies. Even so, we cannot ignore the contributions of such cropland expansion to increasing local income, alleviating poverty, and solving food security of some population in the tropical counties. In contrast, cropland expansion in the temperate usually gained more agricultural productivity compared to that in the tropics. In this study, we also found that Eastern Asia, Southern Asia, Western Asia, Northern America, and Central America and Caribbean locating in the temperate performed positive NPP bias, suggesting increased the productivity compared to those of previous land use types.

Although cropland expansion in some regions increased NPP

compared to earlier land use types, the increases are based on more water resource consumption. Expanded croplands in Eastern Asia, Central Asia, Southern Asia, Western Asia, Southern Africa, Northern Africa, and Central America and Caribbean performed positive NPP bias in this study, but also performed positive ET bias. Note that most of those regions are, however, in water-limited and rainfed areas. It potentially increased the stress of local water resource supply and reshaped the water balance between human and land (Feng et al., 2016). In contrast, cropland expansion in some regions decreased NPP and land cover fraction, e.g., Southern Asia, Eastern Europe, Western Europe, Northern Europe, Eastern Africa, and Southern America, and decreased water resource consumption. However, in this case more precipitation, not used by vegetation, could become land surface runoff. It possibly increased the potential risk of soil erosion, and further resulted in land degradation. Before 1950 s, large-area cropland expansion exerted in the Loess Plateau, which led to severe soil erosion and ecosystem degradation (Chen et al., 2015). Although some ecological engineering measures were successively implemented in the Loess Plateau from 1950 s up to date and gained the expected results, it could be still a long-run way to recover previous good-health ecosystems (Wang et al., 2016).

Considering more cropland expansion occurring on fragile ecosystems and exerting substantial pressures on natural ecosystems, some studies focused on sparing land for nature and cropland intensification (Ewers et al., 2009; Folberth et al., 2020; Gerten et al., 2020; Godfray et al., 2010; Mueller et al., 2012). For example, a recent study based on crop modelling showed that closing current yield gaps by spatially optimizing fertilizer inputs could reduce the ~50% current cropland area (Folberth et al., 2020). Some earlier studies also suggested to close the yield gaps through nutrient and water managements (Jägermeyr et al., 2016; Mueller et al., 2012). Anyhow, current population growth, urbanization expansion and climate change gave more pressures on both global and regional agriculture development (Gornall et al., 2010; Liu et al., 2021; Ortiz-Bobea et al., 2021). Sustainable intensification, producing more food from the same land area while decreasing the environmental impacts, is required (d'Amour et al., 2017; Godfray et al., 2010). Policies could play more important role in future cropland conservation and development.

## 5. Conclusions

Based on satellite-based MODIS NPP, ET, and land cover data, as well as ERA5 precipitation and temperature data, this study used the space-for-time substitution technique, assuming that spatial and temporal variations are equivalent, to investigate the impacts of cropland expansion on agricultural productivity and water source consumption. This study found that global cropland area presented a significant net increasing trend with  $1.9 \times 10^4 \text{ km}^2/\text{a}$  ( $p < 0.01$ ) over the past two decades. Large-area cropland expansion mainly focused on Eastern Asia, Southern Asia, Eastern Europe, Southern America, and Northern America. Global cropland expansion caused average NPP decrease and average ET decrease of new cultivated land pixels, but difference performances were evidently observed in subregions. Cropland expansion in the Southern America performed the strongest NPP and ET decreases. In contrast, expanded cropland in most subregions of Asia and Northern America had higher the agriculture productivity compared to their original land use types, while the increases were done at the expense of more water resource consumption. Although cropland expansion only slightly decreased NPP compared to original ecosystems globally, expanded croplands often occurred in water-limited or temperature-limited areas. It could easily increase the risks of land degradation and abandonment under climate change and less agricultural managements (e.g., irrigation). Considering the lower production ability of the new expanded croplands, improving the intensification of high-quality croplands could be more benefit for meeting the food requirements in the context of increasing population and protecting natural ecosystems.

## Declaration of Competing Interest

The authors declare that they have no known competing financial interests or personal relationships that could have appeared to influence the work reported in this paper.

## Acknowledgements

We are grateful for MODIS NPP, ET, land cover data, and ERA5 precipitation and air temperature data. This study is funded by the National Natural Science Foundation of China (Grant No. 41971218), and the Strategic Priority Research Program of the Chinese Academy of Sciences, China (Grant No. XDA23070302, XDA28130400).

## Appendix A. Supporting information

Supplementary data associated with this article can be found in the online version at doi:10.1016/j.agee.2021.107630.

## References

- Chen, Y., Wang, K., Lin, Y., Shi, W., Song, Y., He, X., 2015. Balancing green and grain trade. *Nat. Geosci.* 8, 739–741.
- d'Amour, B.C., Reitsma, F., Baiocchi, G., Barthel, S., Güneralp, B., Erb, K.-H., Haberl, H., Creutzig, F., Seto, K.C., 2017. Future urban land expansion and implications for global croplands. *Proc. Natl. Acad. Sci. U.S.A.* 114 (34), 8939–8944.
- Dong, J., Xiao, X., Zhang, G., Menarguez, M.A., Choi, C.Y., Qin, Y., Luo, P., Zhang, Y., Moore, B., 2016. Northward expansion of paddy rice in northeastern Asia during 2000–2014. *Geophys. Res. Lett.* 43 (8), 3754–3761.
- Ewers, R.M., Scharlemann, J.P.W., Balmford, A., Green, R.E., 2009. Do increases in agricultural yield spare land for nature? *Glob. Change Biol.* 15 (7), 1716–1726.
- Feng, X., Fu, B., Piao, S., Wang, S., Ciais, P., Zeng, Z., Lü, Y., Zeng, Y., Li, Y., Jiang, X., Wu, B., 2016. Revegetation in China's Loess Plateau is approaching sustainable water resource limits. *Nat. Clim. Change* 6, 1019–1022.
- Folberth, C., Khabarov, N., Balković, J., Skalský, R., Visconti, P., Ciais, P., Janssens, I.A., Peñuelas, J., Obersteiner, M., 2020. The global cropland-sparing potential of high-yield farming. *Nat. Sustain.* 3 (4), 281–289.
- Foley, J.A., DeFries, R., Asner, G.P., Barford, C., Bonan, G., Carpenter, S.R., Chapin, F.S., Coe, M.T., Daily, G.C., Gibbs, H.K., 2005. Global consequences of land use. *Science* 309 (5734), 570–574.
- Foley, J.A., Ramankutty, N., Brauman, K.A., Cassidy, E.S., Gerber, J.S., Johnston, M., Mueller, N.D., O'Connell, C., Ray, D.K., West, P.C., Balzer, C., Bennett, E.M., Carpenter, S.R., Hill, J., Monfreda, C., Polasky, S., Rockström, J., Sheehan, J., Siebert, S., Tilman, D., Zaks, D.P.M., 2011. Solutions for a cultivated planet. *Nature* 478 (7369), 337–342.
- Friedl, M.A., McIver, D.K., Hodges, J.C.F., Zhang, X.Y., Muchoney, D., Strahler, A.H., Woodcock, C.E., Gopal, S., Schneider, A., Cooper, A., Baccini, A., Gao, F., Schaaf, C., 2002. Global land cover mapping from MODIS: algorithms and early results. *Remote Sens. Environ.* 83 (1–2), 287–302.
- Gerten, D., Heck, V., Jägermeyr, J., Bodirsky, B.L., Fetzer, I., Jalava, M., Kumm, M., Lucht, W., Rockström, J., Schaphoff, S., Schellhuber, H.J., 2020. Feeding ten billion people is possible within four terrestrial planetary boundaries. *Nat. Sustain.* 3 (3), 200–208.
- Godfray, H.C.J., Beddington, J.R., Crute, I.R., Haddad, L., Lawrence, D., Muir, J.F., Pretty, J., Robinson, S., Thomas, S.M., Toulmin, C., 2010. Food security: the challenge of feeding 9 billion people. *Science* 327 (5967), 812–818.
- Gornall, J., Betts, R., Burke, E., Clark, R., Camp, J., Willett, K., Wiltshire, A., 2010. Implications of climate change for agricultural productivity in the early twenty-first century. *Philos. Trans. R. Soc. B: Biol. Sci.* 365 (1554), 2973–2989.
- Gu, F., Zhang, Y., Huang, M., Tao, B., Liu, Z., Hao, M., Guo, R., 2017. Climate-driven uncertainties in modeling terrestrial ecosystem net primary productivity in China. *Agric. Meteorol.* 246, 123–132.
- Iizumi, T., Ramankutty, N., 2015. How do weather and climate influence cropping area and intensity? *Glob. Food Secur.* 4, 46–50.
- Jägermeyr, J., Gerten, D., Schaphoff, S., Heinke, J., Lucht, W., Rockström, J., 2016. Integrated crop water management might sustainably halve the global food gap. *Environ. Res. Lett.* 11 (2), 025002.
- Jiang, C., Ryu, Y., 2016. Multi-scale evaluation of global gross primary productivity and evapotranspiration products derived from breathing earth system simulator (BESS). *Remote Sens. Environ.* 186, 528–547.
- Kuang, W., Liu, J., Tian, H., Shi, H., Dong, J., Song, C., Li, X., Du, G., Hou, Y., Lu, D., Chi, W., Pan, T., Zhang, S., Hamdi, R., Yin, Z., Yan, H., Yan, C., Wu, S., Li, R., Yang, J., Dou, Y., Wu, W., Liang, L., Xiang, B., Yang, S., 2021. Cropland redistribution to marginal lands undermines environmental sustainability. *Natl. Sci. Rev.*
- Lesk, C., Rowhani, P., Ramankutty, N., 2016. Influence of extreme weather disasters on global crop production. *Nature* 529 (7584), 84–87.
- Li, W., Buitenwerf, R., Munk, M., Aмоke, I., Bocher, P.K., Svenning, J.-C., 2020a. Accelerating savanna degradation threatens the Maasai Mara socio-ecological system. *Glob. Environ. Change* 60, 102030.



- Li, W., Buitenwerf, R., Munk, M., Bøcher, P.K., Svenning, J.-C., 2020b. Deep-learning based high-resolution mapping shows woody vegetation densification in greater Maasai Mara ecosystem. *Remote Sens. Environ.* 247, 111953.
- Liu, X., Liu, Y., Liu, Z., Chen, Z., 2021. Impacts of climatic warming on cropping system borders of China and potential adaptation strategies for regional agriculture development. *Sci. Total Environ.* 755, 142415.
- Liu, Z., Liu, Y., 2018. Does anthropogenic land use change play a role in changes of precipitation frequency and intensity over the Loess Plateau of China? *Remote Sens.* 10 (11), 1818.
- Liu, Z., Liu, Y., Li, Y., 2019. Extended warm temperate zone and opportunities for cropping system change in the Loess Plateau of China. *Int. J. Climatol.* 39 (2), 658–669.
- Liu, Z., Shao, Q., Liu, J., 2015. The performances of MODIS-GPP and -ET products in China and their sensitivity to input data (FPAR/LAI). *Remote Sens.* 7 (1), 135–152.
- Liu, Z., Wang, J., Wang, X., Wang, Y., 2020. Understanding the impacts of 'Grain for Green' land management practice on land greening dynamics over the Loess Plateau of China. *Land Use Policy* 99, 105084.
- Lobell, D.B., Burke, M.B., Tebaldi, C., Mastrandrea, M.D., Falcon, W.P., Naylor, R.L., 2008. Prioritizing climate change adaptation needs for food security in 2030. *Science* 319 (5863), 607–610.
- Matsushita, B., Xu, M., Chen, J., Kameyama, S., Tamura, M., 2004. Estimation of regional net primary productivity (NPP) using a process-based ecosystem model: how important is the accuracy of climate data? *Ecol. Model.* 178 (3), 371–388.
- Mo, X., Liu, S., Lin, Z., Guo, R., 2009. Regional crop yield, water consumption and water use efficiency and their responses to climate change in the North China plain. *Agric. Ecosyst. Environ.* 134 (1), 67–78.
- Mu, Q., Zhao, M., Kimball, J.S., McDowell, N.G., Running, S.W., 2012. A remotely sensed global terrestrial drought severity index. *B. Am. Meteorol. Soc.* 94 (1), 83–98.
- Mu, Q., Zhao, M., Running, S.W., 2011. Improvements to a MODIS global terrestrial evapotranspiration algorithm. *Remote Sens. Environ.* 115 (8), 1781–1800.
- Mueller, N.D., Gerber, J.S., Johnston, M., Ray, D.K., Ramankutty, N., Foley, J.A., 2012. Closing yield gaps through nutrient and water management. *Nature* 490 (7419), 254–257.
- Niu, Z., Wang, L., Chen, X., Yang, L., Feng, L., 2021. Spatiotemporal distributions of pan evaporation and the influencing factors in China from 1961 to 2017. *Environ. Sci. Pollut. Res.*
- Ortiz-Bobea, A., Ault, T.R., Carrillo, C.M., Chambers, R.G., Lobell, D.B., 2021. Anthropogenic climate change has slowed global agricultural productivity growth. *Nat. Clim. Change* 11 (4), 306–312.
- Pickett, S.T.A., 1989. Space-for-time substitution as an alternative to long-term studies. In: Likens, G.E. (Ed.), *Long-Term Studies in Ecology: Approaches and Alternatives*. Springer New York, New York, NY, pp. 110–135.
- Running, S.W., Nemani, R.R., Heinsch, F.A., Zhao, M., Reeves, M., Hashimoto, H., 2004. A continuous satellite-derived measure of global terrestrial primary production. *Bioscience* 54 (6), 547–560.
- Schmidhuber, J., Tubiello, F.N., 2007. Global food security under climate change. *Proc. Natl. Acad. Sci. U.S.A.* 104 (50), 19703–19708.
- Tan, M., Li, Y., 2019. Spatial and temporal variation of cropland at the global level from 1992 to 2015. *J. Resour. Ecol.* 10 (3), 235–245.
- Tao, F., Yokozawa, M., Hayashi, Y., Lin, E., 2003. Future climate change, the agricultural water cycle, and agricultural production in China. *Agric. Ecosyst. Environ.* 95 (1), 203–215.
- Wang, S., Fu, B., Piao, S., Lü, Y., Ciais, P., Feng, X., Wang, Y., 2016. Reduced sediment transport in the Yellow River due to anthropogenic changes. *Nat. Geosci.* 9 (1), 38–41.
- West, P.C., Gibbs, H.K., Monfreda, C., Wagner, J., Barford, C.C., Carpenter, S.R., Foley, J. A., 2010. Trading carbon for food: Global comparison of carbon stocks vs. crop yields on agricultural land. *Proc. Natl. Acad. Sci. U.S.A.* 107 (46), 19645–19648.
- Yan, H., Fu, Y., Xiao, X., Huang, H.Q., He, H., Ediger, L., 2009. Modeling gross primary productivity for winter wheat–maize double cropping system using MODIS time series and CO<sub>2</sub> eddy flux tower data. *Agric. Ecosyst. Environ.* 129 (4), 391–400.
- Zaveri, E., Russ, J., Damania, R., 2020. Rainfall anomalies are a significant driver of cropland expansion. *Proc. Natl. Acad. Sci. U.S.A.* 117 (19), 10225–10233.
- Zhao, M., Heinsch, F.A., Nemani, R.R., Running, S.W., 2005. Improvements of the MODIS terrestrial gross and net primary production global data set. *Remote Sens. Environ.* 95 (2), 164–176.